



HAL
open science

Hollow-core fiber-based curvature sensor with high sensitivity and large dynamic range

Jonas H Osório, Frédéric Gérôme, Foued Amrani, Fetah Benabid, Frédéric Delahaye, Cristiano M B Cordeiro

► **To cite this version:**

Jonas H Osório, Frédéric Gérôme, Foued Amrani, Fetah Benabid, Frédéric Delahaye, et al.. Hollow-core fiber-based curvature sensor with high sensitivity and large dynamic range. SBFoton International Optics and Photonics Conference, Nov 2024, Salvador, Brazil. pp.TS-WED-C2-1. hal-04744192

HAL Id: hal-04744192

<https://hal.science/hal-04744192v1>

Submitted on 18 Oct 2024

HAL is a multi-disciplinary open access archive for the deposit and dissemination of scientific research documents, whether they are published or not. The documents may come from teaching and research institutions in France or abroad, or from public or private research centers.

L'archive ouverte pluridisciplinaire **HAL**, est destinée au dépôt et à la diffusion de documents scientifiques de niveau recherche, publiés ou non, émanant des établissements d'enseignement et de recherche français ou étrangers, des laboratoires publics ou privés.

Hollow-core fiber-based curvature sensor with high sensitivity and large dynamic range

Jonas H. Osório
Department of Physics
Federal University of Lavras
Lavras, Brazil
jonas.osorio@ufla.br

Foued Amrani
XLIM Institute, CNRS UMR 7252
University of Limoges
Limoges, France
fouedamrani@glophotonics.fr

Frédéric Delahaye
XLIM Institute, CNRS UMR 7252
University of Limoges
Limoges, France
fredericdelahaye@glophotonics.fr

Frédéric Gérôme
XLIM Institute, CNRS UMR 7252
University of Limoges
Limoges, France
frederic.gerome@xlim.fr

Fetah Benabid
XLIM Institute, CNRS UMR 7252
University of Limoges
Limoges, France
f.benabid@xlim.fr

Cristiano M. B. Cordeiro
Institute of Physics Gleb Wataghin
University of Campinas
Campinas, Brazil
cmbc@ifi.unicamp.br

Abstract—We study the application of a tubular-lattice hollow-core fiber displaying thin cladding tubes as a high-sensitivity and large-dynamic range curvature sensor. The device working principle is based on bending-induced core and cladding modes couplings occurring at specific wavelengths and at specific curvature radii. Our characterizations allowed us to determine a sensitivity of $(29.3 \pm 0.4) \text{ nm/m}^{-1}$ for a curvature variation range of 17 m^{-1} . These figures are high when compared with other curvature sensors based on different optical fiber-based sensing configurations. We understand that our work provides a valid path for achieving new hollow-core curvature sensors with enhanced sensitivity and large dynamic range.

Keywords—hollow-core fiber, photonic crystal fiber, fiber sensor, curvature sensor

I. INTRODUCTION

Hollow-core photonic crystal fibers (HCPCFs) stand for a family of microstructured optical fibers able to transmit light through an empty core [1]. Besides being excellent platforms for beam delivery and nonlinear optics applications [2], these fibers show themselves as an enabling technology for the development of new fiber sensors. Indeed, thanks to the possibility of tailoring the HCPCFs' cladding characteristics so as to attain specific guidance properties (*e.g.*, cladding design and geometrical dimensions), a great variety of HCPCF-based sensors have been demonstrated recently. Curvature, temperature, and displacement are examples of parameters that HCPCFs are able to monitor [3].

Specifically, in the realm of curvature sensors, we identify two promising possibilities for accomplishing HCPCF-based bending sensing devices, both of them relying on exploring couplings between core and cladding modes supported by the fiber microstructure. As a first approach, we mention the possibility of exploring the couplings between the fiber core and cladding modes supported by the silica struts in tubular HCPCFs at their resonant wavelengths. To do so, azimuthally asymmetric tubular HCPCFs can be employed and, by using the fact that when an optical fiber is bent the electric field distributions of the modes are spatially shifted (causing the core modes' distribution to get closer or farther from selected cladding tubes), a curvature sensor can be obtained [4]. This is so because the spatial shift of the mode intensity distributions readily impacts the couplings between the core and cladding modes and the corresponding spectral positions of the transmission resonances [4]. Remarkably, if a suitable calibration routine is used, this sensing approach can be used to monitor both the radius and angle of the curvature applied to the fiber [5].

As a second promising approach for sensing curvature using HCPCFs, we mention the possibility of assessing the couplings of core and airy cladding modes by bending the fiber at a specific radius, identified as critical radius [6, 7]. In these situations, the bending applied to the fiber can phase-match the fundamental mode guided in the core and the fundamental airy mode supported by the fiber cladding tubes, hence providing strong mode coupling. As a result, one induces a transmission resonance whose spectral position is dependent on the curvature applied to the fiber. This approach has been theoretically explored with nested-tubes HCPCFs [8] and experimentally investigated using hybrid-lattice HCPCFs [9].

In this context, in this work, we use a tubular HCPCF displaying thin cladding tubes to attain a high-sensitivity and large-dynamic range curvature sensor. The device's principle of operation is based on exploring the bend-induced core and airy cladding modes couplings at the critical radius and on following the spectral shift of the corresponding spectral resonance as a function of the curvature variation. Our efforts allowed us to demonstrate a sensitivity of $(29.3 \pm 0.4) \text{ nm/m}^{-1}$, accounted for a curvature variation range of 17 m^{-1} . Indeed, the measured sensitivity and dynamic range are large when compared with other curvature sensors based on different fiber-based sensing schemes. We recognize that our research offers a promising approach to developing new hollow-core fiber-based curvature sensors with improved sensitivity and extended dynamic range.

II. FIBER STRUCTURE AND SPECTRAL CHARACTERIZATION OF THE BEND-INDUCED RESONANCES

Fig. 1a shows the cross-section of the fiber we use herein. It stands for a tubular HCPCF with a microstructure formed by six cladding tubes with a thickness of 220 nm and a diameter of 22 μm . The cladding tubes define a hollow core with a 33 μm diameter. In this fiber, the ratio between the core and cladding tubes diameters (~ 0.67) has been designed for having an effective singlemode operation via resonant filtering of the core high-order modes [10, 11]. The fiber's outer diameter is 195 μm .

The fiber transmission spectrum is shown in Fig. 1b. Due to its thin cladding tubes, this fiber exhibits a very broad transmission band spanning from 650 nm to 1750 nm (which is the detection limit of our optical spectrum analyzer). This property allows us to explore the curvature response of the fiber over a large spectral range, which readily entails an extended dynamic range for the sensing device when compared to other configurations.

The authors thank FAPEMIG (grants RED-00046-23 and APQ-00197-24), CNPq (grants 309989/2021-3 and 305024/2023-0), and FAPESP (grant 2024/02995-4) for financial support.

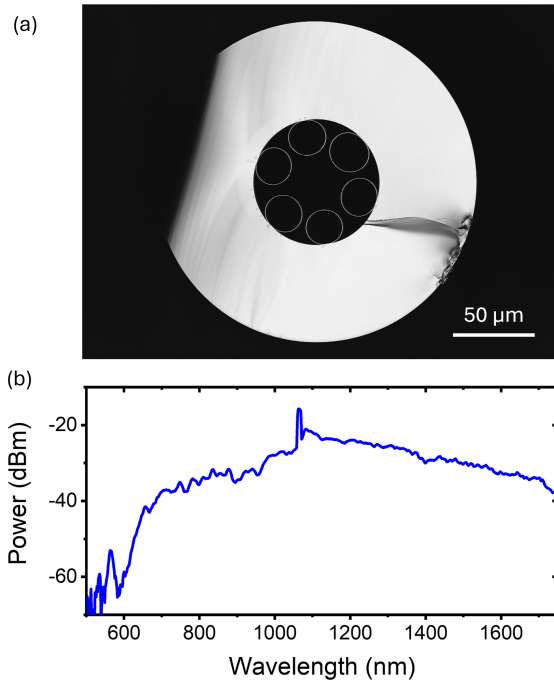


Fig. 1. (a) Fiber cross-section and (b) its corresponding transmission spectrum between 500 nm and 1750 nm. The cladding tubes are 220 nm thick and the fiber transmission band spans from 650 nm to 1750 nm.

When a hollow-core fiber with a tubular lattice is bent, the change in the effective refractive index of the core mode due to the bending can result in phase-matching and resonant coupling to the airy modes supported by the tubular structure [6, 7]. This coupling occurs at a specific curvature radius, known as critical radius, R_{cr} , which can be described by Eq. (1) for the scenario in which the coupling happens between the core fundamental mode and the fundamental mode of the cladding tubes, and with the curvature applied along the direction of one of the cladding tubes. In Eq. (1), D_{core} represents the fiber core diameter, d_{in} is the inner diameter of the cladding tubes, λ is the wavelength, and $u_{01} = 2.405$ is the first root of the zeroth-order Bessel function of the first kind [6, 7].

$$R_{cr} = \frac{\pi^2 D_{core} d_{in}^2}{\lambda^2 u_{01}^2} \left[1 - \frac{d_{in}}{D_{core}} \right]^{-1} \quad (1)$$

By examining Eq. (1), we can see that bending the fiber at a radius R_{cr} will result in coupling between the modes in the core and the cladding tubes around a specific wavelength λ . Since the modes guided through the cladding tubes typically experience higher loss compared to the core fundamental mode, a transmission dip is expected to appear around this wavelength. In turn, if the bending radius is then changed from R_{cr} , the transmission dip is anticipated to shift, enabling the platform to act as a curvature sensor.

To evaluate the performance of the sensing method described here, we used the experimental setup shown in Fig. 2a. Under this approach, light from a supercontinuum source (SC) was directed into the HCPCF (4 m length) using alignment mirrors (M1 and M2) and a coupling lens (L1). To impose different bending conditions on the fiber, we employed a system with a fixed wall and a movable platform attached to a motorized translation stage. By suitably positioning the HCPCF between the walls and adjusting the motorized translation stage, we were able to change the fiber's

bending radius while observing the corresponding transmission spectrum using an optical spectrum analyzer (OSA).

Fig. 2b shows the fiber normalized transmission spectrum (*i.e.*, the difference between the transmission spectrum corresponding to the bent fiber and that corresponding to the straight fiber) for representative curvature radii measured from 1100 nm to 1750 nm. Observation of the plot in Fig. 2b readily allows identifying that bending the fiber induces a transmission dip whose spectral position is redshifted as the curvature radius is reduced.

Fig. 3c displays the wavelengths of such transmission dips as a function of the critical bending radius. Additionally,

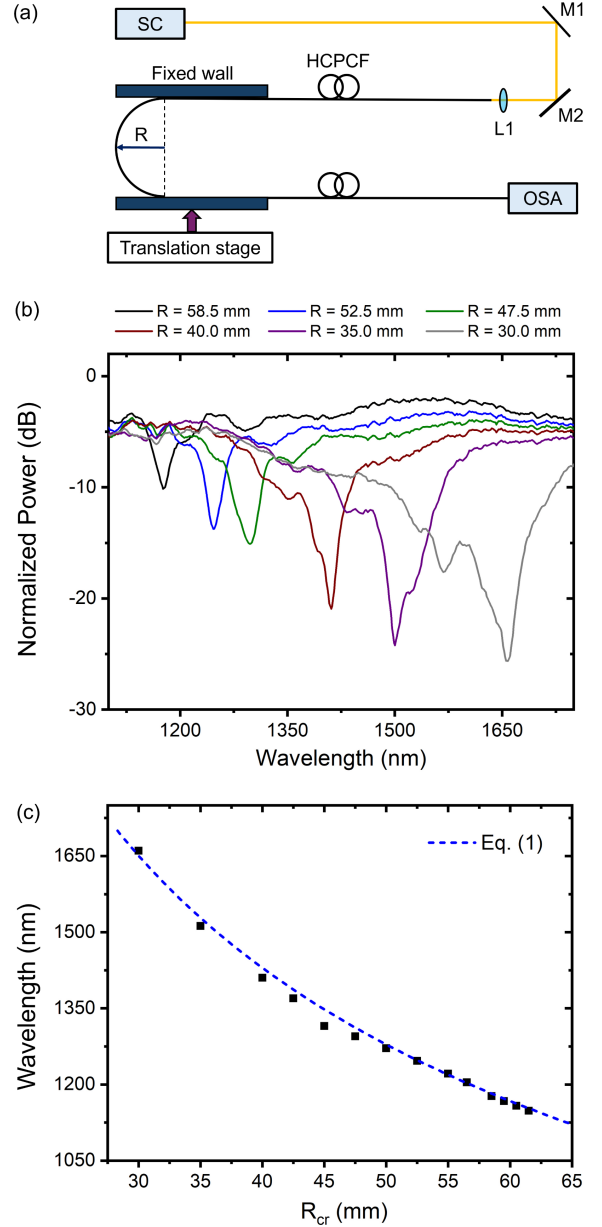


Fig. 2. (a) Diagram of the experimental setup. SC: supercontinuum source. M1 and M2: mirrors. OSA: optical spectrum analyzer. (b) Transmission spectrum (normalized power) for representative curvature radii (R) measured from 1100 nm to 1750 nm. (c) Spectral positions of the bend-induced resonances as a function of the critical radius (R_{cr}). The dashed blue curve indicates the trend line calculated from Eq. (1) using the geometrical parameters of the fiber.

Fig. 2c includes a dashed blue line representing the trend of transmission dip variation with curvature radius calculated using Eq. (1) and the fiber's geometrical parameters. Remarkably, the results derived from Eq. (1) are in very good agreement with the experimental data.

Additionally, we note that the curvature radius variation measured in this work ($\Delta R_{cr} = 32$ mm) is more than 5 times larger than that measured in our previous demonstration using a hybrid-lattice HCPCF [9]. In this framework, we indicate that such significant enhancement in the sensing dynamic range has been enabled by the wide transmission band of the tubular HCPCF employed in this study. Notably, in our experiments, the bend-induced transmission dip is shifted by approximately 500 nm as the bending radius decreased from 61.5 mm to 30 mm. Thus, the broad bandwidth of the HCPCF has allowed for extending the curvature radius range that the platform is capable of detecting. In the next section, we determine the device's sensitivity and compare it with other fiber-based curvature sensors.

III. SENSITIVITY AND DYNAMIC RANGE ANALYSIS

In curvature sensing measurements, one typically defines the curvature parameter, C , as in Eq. (2), in which R is the radius of the bending applied to the fiber. By accounting for the wavelength shift as a function of the curvature parameter, we can determine the device sensitivity in units of nm/m^{-1} .

$$C = \frac{1}{R} \quad (2)$$

Thus, by using the above-mentioned curvature definition, we can build the plot shown in Fig. 3, which displays the wavelength shift of the transmission dips, $\Delta\lambda$, as a function of the variation of the curvature parameter, ΔC . Here, we define $\Delta\lambda = \lambda_i - \lambda_0$, where λ_i is the spectral position of the resonant dip corresponding to a certain curvature radius R_i . In turn, we set $\lambda_0 = 1148.3$ nm, which stands for the spectral position corresponding to the curvature radius of $R_0 = 61.5$ mm ($C_0 \sim 16.3 \text{ m}^{-1}$), the largest bending radius considered in the measurements shown in Fig. 2c. The variation of the curvature parameter, ΔC , has been calculated by making $\Delta C = C_i - C_0$, where $C_i = 1/R_i$.

Observation of the plot in Fig. 3 allows for recognizing a nearly linear trend for the dataset corresponding to $\Delta\lambda$ as a function of ΔC (coefficient of determination, r^2 , equals 0.99776). Thus, by linear fitting the data in Fig. 3, we can determine our sensor's sensitivity as $(29.3 \pm 0.4) \text{ nm}/\text{m}^{-1}$. Remarkably, this sensitivity value is higher than those measured using other curvature sensors based on different fiber technologies such as Bragg gratings in surface-core fibers [12] and interferometers [13, 14]. Additionally, we mention that the dynamic range demonstrated for our configuration, namely 17 m^{-1} , is larger than that measured for other fiber sensing configurations including our previous demonstration using a hybrid HCPCF [9], and other technologies such as surface-core fibers [12] and multimode interference [15].

IV. CONCLUSIONS

In this work, we investigated a curvature sensing platform based on a tubular HCPCF displaying thin cladding tubes. Characterization of the sensing setup has allowed us to estimate a sensitivity of $(29.3 \pm 0.4) \text{ nm}/\text{m}^{-1}$, which is higher than that measured for other fiber technologies based on, for example, Bragg gratings and interferometers. Additionally, we could demonstrate our sensor operation over a large

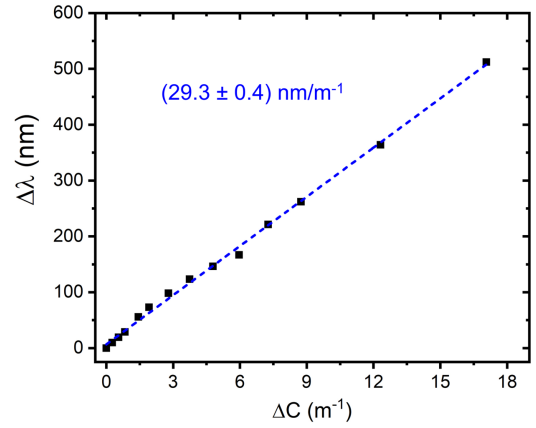


Fig. 3. Wavelength shift ($\Delta\lambda$) versus the curvature variation (ΔC). The dashed blue line has been obtained by linear fitting the measured dataset. The sensitivity has been calculated as $(29.3 \pm 0.4) \text{ nm}/\text{m}^{-1}$.

dynamic range (17 m^{-1}). Thus, considering that achieving high sensitivity and large dynamic range in the same fiber sensing configuration is typically a challenging task, we believe that our work provides a promising route for creating new hollow-core fiber-based curvature sensors with enhanced sensitivity and a broader dynamic range, hence contributing to the wider scenario of fiber curvature sensing technologies.

REFERENCES

- [1] J. H. Osório *et al.*, "Hollow-core fibers with reduced surface roughness and ultralow loss in the short-wavelength range," *Nature Communications*, 14, 1146, 2023.
- [2] B. Debord *et al.*, "Hollow-core fiber technology: the rising of gas photonics," *Fibers* 7, 2, 2019.
- [3] J. H. Osório, C. M. B. Cordeiro, "Hollow-core fiber-based sensors: recent advancements in Brazil," 2024 Latin American Workshop on Optical Fiber Sensors (LAWOFS), 1-2, 2024.
- [4] C. M. B. Cordeiro *et al.*, "Azimuthally asymmetric tubular lattice hollow-core optical fiber," *JOSA B*, 38, 12, F23-F28, 2021.
- [5] W. M. Guimarães *et al.*, "Angle-resolved hollow-core fiber-based curvature sensing approach," *Fibers* 9, 72, 2021.
- [6] M. H. Frosz *et al.*, "Analytical formulation for the bend loss in single-ring hollow-core photonic crystal fibers," *Photon. Res.*, 5, 88-91, 2017.
- [7] R. M. Carter *et al.*, "Measurement of resonant bend loss in anti-resonant hollow core optical fiber," *Optics Express*, 25, 20612-20612, 2017.
- [8] C. Wei *et al.*, "Directional bending sensor using negative curvature fibers with asymmetric nested cladding tubes," 2022 IEEE Photonics Conference, 1-2, 2022.
- [9] A. D. P. Souza *et al.*, "Curvature sensing with a hybrid-lattice hollow-core photonic crystal fiber," 2023 International Conference on Optical MEMS and Nanophotonics and SBFoton International Optics and Photonics Conference, 1-2, 2023.
- [10] P. Uebel *et al.*, "Broadband robustly single-mode hollow-core PCF by resonant filtering of higher-order modes," *Optics Letters* 41, 1961-1964, 2016.
- [11] F. Amrani *et al.*, "Low-loss single-mode hybrid-lattice hollow-core photonic-crystal fibre," *Light: Science & Applications* 10, 7, 2021.
- [12] J. H. Osório *et al.*, "Bragg gratings in surface-core fibers: refractive index and directional curvature sensing," *Optical Fiber Technology*, 34, 86-90, 2017.
- [13] H. Fu *et al.*, "High-Sensitivity Mach-Zehnder Interferometric Curvature Fiber Sensor Based on Thin-Core Fiber," *IEEE Sensors Journal*, 15, 1, 520-525, 2015.
- [14] S. Dong *et al.*, "High Sensitivity Optical Fiber Curvature Sensor Based on Cascaded Fiber Interferometer," *Journal of Lightwave Technology*, 36, 4, 1125-1130, 2018.
- [15] W. Yang *et al.*, "Fiber-optic multimode interferometric curvature sensor based on small-inner-diameter hollow core fiber," *Optical Fiber Technology*, 67, 102749, 2021.

